International Journal of Modern Engineering Research (IJMER)
www.ijmer.com Vol.3, Issue.4, Jul - Aug. 2013 pp-1857-1860 ISSN: 2249-6645

Optical and Impedance Spectroscopy Study of ZnS Nanoparticles

Ramna Tripathi[1] & Akhilesh Kumar[2]
[1]*Department of Physics, THDC-Institute of Hydropower Engineering & Technology, Tehri, Uttarakhand, India*
[2]*Department of Physics, Government Post Graduate College, Rishikesh, Uttarakhand, India*

Abstract: *Zinc Sulphide particle in the nanometer size regime has been synthesized using chemical routes. The particles were capped using 2-mercaptoethanol to achieve the stability and avoid the coalescence. The as-obtained particles were characterized by X-ray diffraction (XRD), Transmission electron microscopy (TEM), UV–VIS absorption and photoluminescence (PL) spectra. The dielectric measurements of the ceramic were carried out as a function of frequency (100 Hz–1 MHz) and temperature (298–373 K) by impedance spectroscopy. Impedance spectroscopy was employed to determine the electrical parameters (resistance, capacitance and relaxation time) of the grain and the grain boundary. The grain boundary conduction, total grain (grain plus grain boundary) and the frequency max of grain boundary followed an Arrhenius law associated with activation energies of 0.27eV, 0.28 eV and 0.3 eV respectively.*

Keywords- *Chemical synthesis, Impedance spectroscopy, Optical properties, Zinc Sulphide*

I. INTRODUCTION

Zinc Sulphide is a semi-conducting material, with a wide band gap of 3.70 eV [1]. Among the wide band gap materials, luminescent semi-conducting nanocrystals, also termed as nanophosphors, have been paid much attention particularly for their life time shortening and enhanced emission efficiencies [2, 3]. There have been extensive reports in the past few years demonstrating the systematic exploration of growing ZnS nanoparticles in the surfactant system to control the particle size. Tang et al. [4] for example have studied the luminescence and photo physical properties of ZnS nanoparticles prepared by reverse micelle method. During the recent years, various properties of ZnS have been investigated by researchers [5-10].

It is to be mentioned that the impedance spectroscopy is one of the powerful tools for the characterization of electrical properties of semiconducting nanomaterials. AC impedance spectroscopy allows measurement of the capacitance and loss tangent (tan δ) and/or conductance over a frequency range at various temperatures. From the measured capacitance and tan δ, four complex dielectric functions can be computed: impedance (Z*), electric modulus (M*), permittivity (ε*), and admittance (Y*).

II. EXPERIMENTS

Although various methods are available for the synthesis of ZnS nanoparticles, chemical precipitation is widely being used for the preparation of colloidal nanoparticles as the possibility of cluster formation is very less in this method when compared to the other methods. Here, 0.27 g of $ZnCl_2$ (1/10 M, 20ml) solution and 0.1M Na_2S solution were prepared in distilled water and were first refluxed for an hour separately. 50 ml Na_2S solution was then added to the mercaptoethanol solution of 0.25 ml (10^{-2} M) and then 20 ml $ZnCl_2$, which was continuously refluxed to get a colloidal form of ZnS. The colloidal sample was refluxed for another 20 min at 80°C for uniform distribution of the particles. Then this was filtered out and washed with distilled water and ethanol for removing the additional impurities formed during the preparation process. The filtrate was dried at room temperature, which yields high-quality ZnS nanocrystals.

The X-ray diffraction of the sample at room temperature is taken by a powder X-ray diffratometer (Rigaku Miniflex-II). The transmission electron micrograph of the sample is taken by a transmission electron microscope (Jeol JEM-100cx). The absorption and luminescence spectra for ZnS nanoparticles were recorded using UV-Visible spectrophotometer (Shimadzu UV-2450) and spectrofluorometer (Shimadzu RF-5310) respectively.

The dielectric measurement of the sample of thickness 2.06 mm and diameter 10.41 mm was carried out using gold electrodes by an LCR meter (Hioki) in the frequency range from 100 Hz to 1 MHz and in the temperature range from 298 K to 373 K. The temperature was controlled with a programmable oven. All the dielectric data were collected while heating at a rate of 1^0C min^{-1}. The complex electric modulus M^* ($=1/\varepsilon^*$) and impedance Z^* ($=M^*/j\omega C_o$) are obtained from the temperature dependence of the real (ε') and imaginary (ε") components of the dielectric permittivity ε^* ($= \varepsilon'-j\varepsilon''$) and $\varepsilon''= \varepsilon' \tan\delta$.

III. RESULTS AND DISCUSSION

Fig. 1 shows the X-ray diffraction pattern of the sample taken at room temperature. The broadening of the diffraction peaks is primarily due to the finite size of the nanocrystallites and is quantitatively analyzed by the Debye–Scherrer formula

$$L = \frac{0.94\lambda}{B\cos\theta} \qquad (1)$$

where L is the average size of the particle, λ is the wavelength of X-ray radiation, B is the full width at half maximum (FWHM) and θ is the diffraction angle. According to the data in Fig. 1 and given formula, the average particle size of the material is found to be 45 nm. The transmission electron micrograph of the ZnS is shown in the inset of Fig. 1. The average grain size of the nanoclusters of ZnS is found to be 50 nm. Particle size analyzed by XRD and TEM are in good agreement.

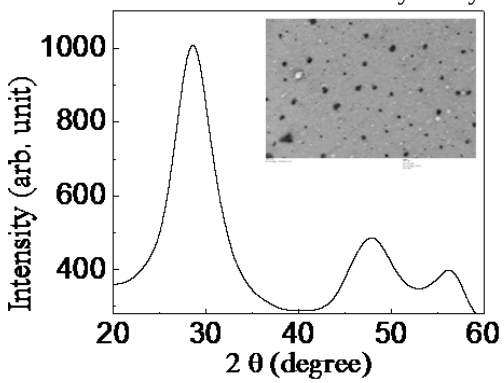

Fig. 1. The XRD (TEM micrograph shown in the inset) for ZnS.

The inset of Fig. 2 shows the UV – visible spectra of ZnS nanoparticles in the absorbance range of 200-350 nm. The absorbance peak at 277 nm is blue shifted compared to the bulk ZnS for which absorption peak is at 345 nm. The blue-shifted absorption edge is due to the quantum confinement of the excitons present in the sample, resulting in a more discrete energy spectrum of the individual nanoparticles. The broadening of the absorption spectrum is mainly due to the quantum confinement of the ZnS nanoparticles. The effect of the quantum confinement on impurity critically depends on the size of the host crystal. As the host decreases, the degree of confinement and its effect increases. The band gap energy is increased (~4.1 eV) compared to that (~3.6 eV) of bulk ZnS shown in the Fig. 2, the enlargement of the band gap can be attributed to the quantum confinement effect of the ZnS nanoparticles.

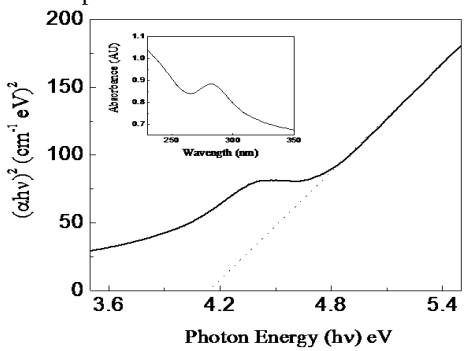

Fig. 2. Energy band gap determination of ZnS nanoparticles. The UV-visible absorption spectra of the ZnS nanoparticles shown in the inset.

Fig. 3 shows the PL emission (a) and excitation (b) spectra of ZnS nanoparticles. It shows strong blue-luminescence with peak maximum around 335 nm and a side band at 352 nm. The corresponding excitation spectra with peak maximum at 420 nm indicate energy-transfer from the band-to-band electronic excitation of the quantum confined ZnS [11].

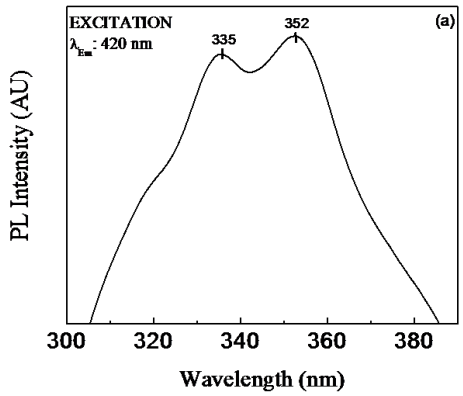

Fig.3. Photoluminescence emission spectra of ZnS nanoparticles.

With the self-aggregation of nanoparticles, the excitation spectra also show reduction in the intensity but more significantly, a gradual red-shift in the peak maximum with larger line broadening. The origin of the blue-luminescence of ZnS nanoparticles has been studied by different groups [11, 12]. Highly asymmetric and broadened emission band with multiple

peak maxima indicate the involvement of different luminescence centers in the radiative process. The nanoparticles prepared under sulphur deficient synthetic condition of S^{2-}/Zn^{2+} will have larger concentration of sulphur vacancies (VS).

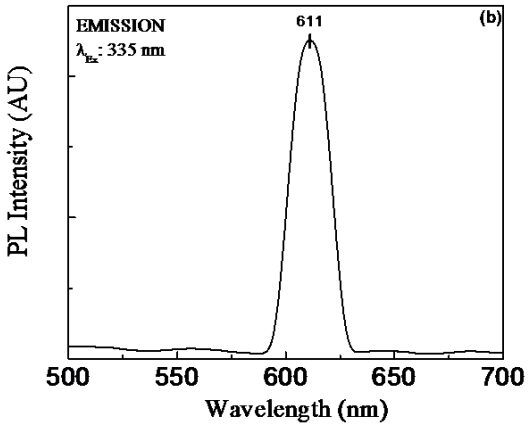

Fig.3. Photoluminescence excitation spectra of ZnS nanoparticles.

It is reported that sulphur vacancies can act as doubly ionized electron trap centers and facilitate VS/VB (valence band) and/or VS/SS (surface states, including interstitial defects and impurities) [11]. Though the lattice vacancies are point defects, due to the large surface-to-volume ratio of nanoparticles, the concentration of these defects will be more at the surface regions than the interiors. Therefore, in the ZnS nanoparticles with unmodified surfaces, the effect of surface states will be dominant as seen by the strong blue luminescence. However, the observed quenching of these emission bands with the self-assembly of nanoparticles suggests that the vacancy centers are annihilated during the particle-to-particle attachment/interface precipitation by way of incorporation of more and more crystal growth units at the nanoparticles surfaces.

Fig. 4 shows a complex-plane impedance plot (Z^*) of ZnS, plotting the imaginary part Z'' against the real part Z'. In general, for a perfect crystal, the values of resistance R and capacitance C can be analyzed by an equivalent circuit of one parallel resistance-capacitance (RC) element. This RC element give rise to one semicircular arc on the complex plane and has intercepts on the Z' axis of zero and R. Thus, C can be calculated with the relation $\omega_m RC=1$, where $\omega_m=2\pi\nu_m$ and ν_m is the frequency at the arc maxima.

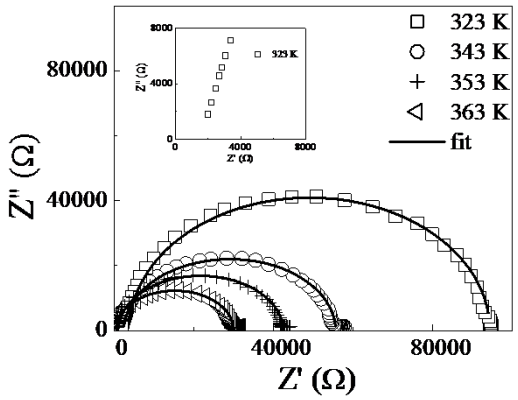

Fig.4. The complex–plane impedance plot with the corresponding equivalent circuit is shown for ZnS at various temperatures. The solid line is the best fit for ZnS. The inset shows expanded views of the high-frequency data near the origin at 323 K.

For a nano crystal containing interfacial boundary layers, the equivalent circuit may be considered as two parallel RC elements connected in serial and giving rise to two arcs in complex plane: one for the nano crystal (grain) and the other for the interfacial boundary (grain-boundary) response. The relative position of the two arcs in the complex plane can be identified by the frequency. Based on the equivalent circuit consisting of two parallel RC elements in series, the nonzero intercept on the Z'-axis (at 323 K) indicates the presence of an arc with ω_{max} higher than the maximum frequency measured (1 MHz).

Dielectric relaxation observed in electroceramics are better analysed using the simplified equivalent circuits consisting of two parallel RC circuits connected in series, one RC element, R_g C_g, representing the grain, and the other $R_{gb}C_{gb}$, representing the grain boundary [13, 14], as shown in the inset of Fig. 4. Here, R_g, C_g and R_{gb}, C_{gb} are the resistance and capacitance associated with the grain and the grain boundary, respectively. Each parallel RC element results in a semicircle in the impedance plots. Fig. 4 shows a complex impedance Z* (Z" versus Z') plot for ZnS nanoceramics, obtained by plotting the imaginary part (Z") against the real part (Z') in the 323 K–363 K temperature range. The high frequency impedance response of the sample in the 323 K–363 K temperature range has been highlighted in Fig. 5 to show the evolution of the high frequency semicircle.

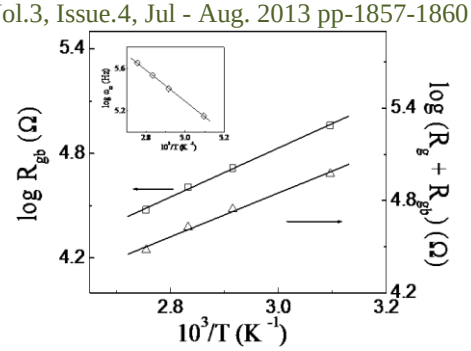

Fig.5. Arrhenius plot for the grain boundary resistance (*R*gb) and total grain. The insetshows grain boundary relaxation frequency (ω_{gb}) for ZnS nanoceramics. The solid line is the best fit for the Arrhenius equations.

The equivalent electrical equation can be represented by

$$Z' = \frac{R_g}{1+(\omega R_g C_g)^2} + \frac{R_{gb}}{1+(\omega R_{gb} C_{gb})^2} \quad (2)$$

$$Z'' = R_g\left(\frac{\omega R_g C_g}{1+(\omega R_g C_g)^2}\right) + R_{gb}\left(\frac{\omega R_{gb} C_{gb}}{1+(\omega R_{gb} C_{gb})^2}\right) \quad (3)$$

The best fitting of RC equivalent circuit by solid line for 323 K, 343 K and 363 K with two semicircular arc of R_g and R_{gb} is shown in the table 1.

The resistance values of the grains and the grain boundaries are obtained from the intercepts of the corresponding semicircles with the real axis (Z') (diameter of each semicircle) which gives R_g and R_{gb}, respectively. The resistance obtained for the total resistance or dc resistance of the sample log $(R_g + R_{gb})$ and log R_{gb} is plotted in the Arrhenius format in the Fig. 5, obey the Arrhenius law with activation energy of 0.28 eV and 0.27 eV respectively. Plot of log (ω_{gb}) (relaxation frequency of grain boundary) (inset of Fig. 5) reveal that ω_{gb} follow an Arrhenius law associated with activation energies of 0.28 eV. Furthermore, as it is clear from Fig. 5, $R_{gb} + R_g$ are only slightly higher than R_{gb} in the entire temperature range under study. Hence, it could be concluded that $R_{gb} >> R_g$, so that in the entire temperature range $C_{gb} >> C_g$.

IV. CONCLUSIONS

The frequency-dependent dielectric dispersion of ZnS nanoparticles synthesized by soft chemical method is investigated in the temperature range from 298 K to 373 K for the first time. The increasing dielectric constant with increasing temperature is attributed to the conductivity which is directly related to an increase in mobility of localized charge carriers. Analyses of the real and imaginary part of complex permittivity with frequency were performed assuming a distribution of relaxation times as confirmed by Cole-Cole plot as well as the scaling behavior of impedance spectra. The scaling behavior of the imaginary part of impedance spectra suggests that the relaxation describes the same mechanism at various temperatures. The frequency-dependent electrical data are also analyzed in the framework of conductivity and modulus formalisms.

ACKNOWLEDGMENT

R. Tripathi and A. Kumar are thankful to Uttarakhand state council of science and technology (U-COST) for its financial support, SAIF, Bose Institute, Kolkata for instrument facility and Gajendra Saini, AIRF, Jawaharlal Nehru University (JNU), New Delhi for TEM measurement.

References

[1] B. S. Zou, R. B. Little, J. P. Wang, M. A. Sayed, Int . J. Quantum Chem. *72* (1999) 439.
[2] R. N. Bhargava, D. Gallangher, Phys.Rev.Lett. *72* (1994) 416.
[3] T. Igarashi, T. Isobe, M. Senna, Phys.Rev.B. *56* (1995) 6444.
[4] H. Tang, G. Y. Xu, L. Q. Weng, L. J. Pan, L. Wang, Acta Mater. *52* (2004) 1489.
[5] M.Y. Nadeem, Waqas Ahmad**,** Turk J Phy, *24* (2000), 651.
[6] R. P. Vijayalakshmi, R. Venugopal, D. R. Reddy, B. Reddy, Physica Scripta. *53* (1996) 123.
[7] K. S. Rathorea, D. Patidara, Y. Janub, N.S. Saxenaa, K. Sharmaa, T. P. Sharmaa, Chalcogenide Lett. 5 (2008) 105.
[8] J. P. Borah, J. Barman, K.C. Sarma, Chalcogenide Lett. *5* (2008) 201.
[9] D. Denzler, M. Olschewski, K. Sattler, J. Appl. Phys. *84* (1998) 2841.
[10] J. Nanda, Sameer Sapra, D. D. Sarma, Chem. Mater. *12* (2000) 1018.
[11] K. Manzoor, S.R. Vadera, N. Kumar, T.R.N. Kutty, Mater. Chem. Phys. *82* (2003) 718.
[12] D. C. Sinclair, A. R. West, J. Appl. Phys. *66* (1989) 3850.
[13] A. M. Macdonald, Impedance Spectroscopy (New York: Wiley), 1987.
[14] A.K. Jonscher, Dielectric Relaxation in Solids, Chelsea Dielectrics Press, London, 1983.
[15] A.K. Jonscher, Universal Relaxation Law, Chelsea Dielectrics Press, London, 1996.
[16] K. S. Cole, R. H. Cole, J. Chem. Phys. *9* (1941) 341.